

Electric Field Variations During Substorms:

OGO-6 Measurements

By

J. P. Heppner
NASA Goddard Space Flight Center
Greenbelt, Maryland

January 1972

*Invited paper given at the Symposium on Morphology and Physics of Magnetospheric Substorms, XV IUGG General Assembly, Moscow, 1971. For publication in the Journal of Planetary and Space Science.

ABSTRACT

The OGO-6 electric field measurements make it clear that the general pattern of high latitude electric fields in magnetic time-invariant latitude coordinates is not highly variable and that when unusual variations, or field distributions, occur they are relatively isolated in time and spatial extent. Thus, electric field changes on a global scale cannot, in general, be evoked as a direct cause of substorms. Polar traverses along the 18^h to 6^h magnetic time meridian show that the sum of potential drops across the evening auroral belt (poleward E) and morning auroral belt (equatorward E) approximately equals the potential drop across the polar cap (dawn-dusk E). The integrated polar cap potential drop ranges from 20 to 100 kev and values in the center of this range (e.g., 40 to 70 kev) are most common under conditions of moderate magnetic disturbance (e.g., Kp = 3). Roughly near 18^h magnetic local time, a latitudinally narrow strip at the transition between auroral belt and polar cap fields exhibits unusually large field fluctuations immediately following the sudden onset of a negative bay at later magnetic local times. It appears likely that this spatially isolated correlation is related to an effect rather than a cause of substorm enhancement. Other indications of direct correlation between electric field behavior and stages of magnetic bay development have not been found to be repeatable for multiple cases. These preliminary studies do not, however, rule out the possibility that more subtle relationships will be found in future studies.

INTRODUCTION

A number of reviews of electric field measurements are currently in press (Haerendel, 1971; Maynard, 1972; Cauffman, 1972) whereas the most comprehensive measurements, those of OGO-6, have not been published. Thus, in place of the review requested by the symposium chairman, presentation of the gross characteristics of high latitude electric fields, as seen in preliminary analyses of OGO-6 data, appears in order. The variations during substorms cannot be discussed until a basis exists for comparing variations at particular times with the general variability observed at times when major substorm changes are not evident. Thus, in this presentation the general character of high latitude electric fields is examined first; next, unusual field distributions are shown; and third, examples during individual substorm events are given. As discussed later, distinctions between substorm fields and fields in general are usually not very meaningful because of the continuous nature of substorms. However, the intensification of activity immediately following times of sudden negative bay onsets is found to be accompanied by an abnormal perturbation in the electric field, apparently isolated to the early evening hours, at the transition between auroral belt and polar cap convective regions. These perturbations are likely to represent effects, rather than initial cause, and as such they are probably not, at this stage of study, as fundamentally important as more general aspects of the field.

It is convenient to refer to the polar region of dawn-dusk electric fields (or anti-solar convection) as the "polar cap," and to refer to the adjacent lower latitude region of poleward (evening) and equatorward (morning) electric fields (or sunward convection at 18^h and 6^h) as the "auroral belt." This convenient nomenclature is not, however, always technically accurate.

For example: (a) aurora can appear in the polar cap region and in the literature one finds the term polar cap aurora, (b) the belt of sunward convection is wider than the instantaneous latitudinal width of the belt where visible aurora is apparent (i.e., visible aurora usually occurs in strips within the "auroral belt convection"), and (c) the boundary between solar and anti-solar convection is sometimes very sharp but more often it is a transition as one would expect in view of convective continuity across the boundary. Despite these difficulties in definition, examination of simultaneous OGO-6 particle data (experiment of D. Evans) and detailed studies (unpublished) of the polar cap-auroral belt transition with Ba⁺ clouds, illustrate that the polar cap-auroral belt convective boundary is frequently the instantaneous high latitude boundary of auroral occurrence. Thus, with awareness that this nomenclature does not fit all times or situations, it is used here. On completion of correlative studies it should be possible to adopt a new nomenclature that will avoid semantic difficulties.

DISTRIBUTION OF OGO-6 DATA

The OGO-6 measurements were made using the double probe floating potential technique originally described by Aggson and Heppner (1964). In addition to dc measurements, the rms signal in each of 5 bands (4-16, 16-64, 64-256, 256-1024, and 1024-4096 Hz) was measured approximately once per second and dc variations with periods < 60 sec were recorded logarithmically at seven samples/sec. For brief periods of real time transmission these rates became multiplied by either 2 or 8. Several samples of the ac (rms) measurements are shown in Maynard and Heppner (1970). Except for the influence of using the logarithmic detector together with the direct dc measurements in designating boundaries, only dc recordings are presented here.

Figure 1 shows the location of the symmetric probes extending outward from the solar panels. The spacecraft was stabilized about all 3-axes such that the measurement axis was always horizontal (i.e., parallel to the earth's surface) and always perpendicular to the direction of the sun. Highly accurate measurements were obtained in initial operation during the interval June 9-22, 1969. A step function change on June 22 exposed solar panel voltages to the ambient plasma and caused the spacecraft potential to jump to a large value. Subsequent to this change measurements were only useable when the satellite was eclipsed from the sun by the earth. Only the June 9-22 measurements are discussed here. During this period the orbit plane was approximately perpendicular to the noon-midnight meridian as illustrated by Figures 2 and 3. This was fortunate for two reasons: (a) in this orientation the quantity $\underline{v}_s \times \underline{B}$, where \underline{v}_s is the satellite velocity, is small in the direction of the X-axis (i.e., the measurement axis) of the spacecraft, and (b) the electric field component measured is dawn-dusk in the polar cap and dominantly N-S at lower latitudes. This means that the measurements are centered on the directions of maximum electric field in the polar cap and at auroral latitudes, as observed in numerous Ba^+ release experiments (Föppl et al., 1968; Wescott et al., 1969, 1970; Haerendel and Lüst, 1970; Heppner et al., 1971).

The high latitude coverage in magnetic coordinates for one days operation is shown in Figure 3. As there are 14 or 15 polar passes each day, in each hemisphere, there are several hundred traverses for study in the June 9-22 interval. Figures 2 and 3 also illustrate that although the north and south polar measurements are distributed, respectively, toward the night and the day hours in magnetic coordinates, the north polar sub-satellite ionosphere

is sunlit whereas the south polar sub-satellite ionosphere is in darkness. The satellite, however, remains in sunlight throughout all orbits during this time interval with perigee and apogee at altitudes near 400 and 1100 kms, respectively, and in middle latitudes.

TYPICAL MEASUREMENTS

(A) Data characteristics

Although the auroral belt field magnitudes are slightly less than average in Figure 4 (top curve), it shows a relatively typical traverse directly across the north magnetic pole. The satellite enters the auroral belt near 18^h 8^m MLT (magnetic local time) and observes a northward (or poleward) electric field. The field reverses ($+ E_X \rightarrow - E_X$) going into the polar cap and remains relatively constant in magnitude while crossing the highest latitude region. The field reverses again ($- E_X \rightarrow + E_X$) on entering the auroral belt near 6^h 26^m MLT. The plus direction in the morning auroral belt is southward (or equatorward).

Figure 4 (bottom curve) shows the south polar measurements from the same orbit. In spacecraft coordinates the sign of E_X in each region is the reverse of the sign in the N. hemisphere. The satellite enters the morning auroral belt near 6^h MLT and observes an equatorward field. The field reverses to the dawn-dusk direction on entering the polar cap and reverses again on entering the evening auroral belt.

In the Figure 4 plots, and all subsequent similar plots, the $(\underline{v}_S \times \underline{B})_X$ field from the satellites velocity \underline{v}_S and the $(\underline{v}_e \times \underline{B})_X$ field from the earth's rotation have been subtracted from the measured values. The zero on each scale is taken from the equatorial crossing points where $(\underline{v}_S \times \underline{B})_X + (\underline{v}_e \times \underline{B})_X = 0$ on the same orbit: the average for the equatorial crossings preceding and following the polar pass plotted is used. These are computer functions; no other corrections have been made on the plots shown here.

The determination of zero's, which means removing contact potentials from the measurements, by the above method usually gives an excellent fit to the lower latitude regions adjoining the auroral belts in the northern hemisphere. The closeness to zero at invariant latitudes (Λ) less than 60° in Figure 4 (top curve) is typical but there are many cases where the displacement in this region is as much as 5 volts/km. The fit between equatorial zero's and measurements taken on the equatorward side of the S. hemisphere auroral belts is not as close as illustrated by Figure 4 (bottom curve). The displacement is rather consistently 5 to 10 volts/km. This offset is presently not fully understood; it could be caused by an error in spacecraft orientation that affects the $\underline{v} \times \underline{B}$ calculation as well as some physical effect (e.g., Aggson, personal communication, has shown that the offset is removed by assuming a slightly different effective antenna length in the two hemispheres). As it is not yet understood it is not corrected here using ad hoc assumptions. The reader is asked to mentally take the offset into account in examining S. hemisphere plots.

It should also be noted that satellite altitude is ignored in the plots shown. For exact comparisons of magnitudes at different locations, or with other measurements, the measurements would need to be referred to a common altitude level by projection along magnetic field lines. If referred to the 100 km level, which has frequently been used as a reference plane in Ba^+ experiments, the maximum magnitude increase would be about 20 percent.

(B) Polar crossings with maximum $\Lambda > 85^\circ$

Comparison of the N. and S. hemisphere passes in Figure 4 also illustrates a frequently encountered physical difference in the data from the two polar regions; that is, the field is conspicuously more irregular in the south polar

pass. This is true even though the pass is to the magnetic nightside of the pole and thus the irregularities cannot be directly related to the dayside field reversals and irregularities discussed later. Although many S. hemisphere polar passes do show a relatively smooth field across the polar cap, it is statistically clear that irregularities are more common in the south polar region than in the north polar region for equivalent magnetic time vs. invariant latitude locations. There are two approaches to explanation: (1) in terms of ionospheric conductivity--noting that the sunlit, more conducting, ionosphere in the N. hemisphere will tend to short out field differences, and (2) in terms of the stresses producing the convection--noting that because of the solstitial tilt of the N. pole toward the sun the uniformity of these stresses may be quite different in the two hemispheres for flux tubes extending to great distances in the magnetospheric tail. The second approach appears most promising but requires considerably more complex magnetospheric modeling than attempted to date.

Figure 5 shows two more passes from roughly 18^h to 6^h MLT across the north magnetic pole. The field magnitudes are greater than in Figure 4 although the 3-hour Kp index is slightly less in Figure 5 (top curve) and slightly greater in Figure 5 (bottom curve). In general, magnitudes do not relate closely to Kp but there is a statistical tendency for the integrated electric field intensity to be greatest when the magnetic disturbance is large, and smallest when the magnetic disturbance is weak. A magnetic index, such as AE, with better time resolution than Kp might give a closer relationship; however, from simple examination of electric field magnitudes relative to the existence of intense magnetic bays, it is obvious that there would be many deviations from statistics. This is consistent with the lack of direct relationships between electric field and magnetic disturbance intensities noted in Ba⁺ drift experiments (Haerendel and Lüst, 1970; Wescott et al., 1970).

A polar traverse at a time when K_p was zero, with no intervals of $K_p > 1$ within 12 hours before or after the traverse, is shown in Figure 6. As the integrated field magnitudes for this traverse are the minimum observed for a pass across the pole, this case fits the statistical tendency, noted above, very well. It also illustrates the pitfall of defining the "polar cap" in terms of measurement thresholds as Frank and Gurnett (1971) have in effect done in terms of Injun-5 electric field data. Although achieving ± 10 volt/km threshold levels in select cases, Injun-5 thresholds of ± 30 volts/km were most common (Cauffman and Gurnett, 1971). Thus, the electric field in a case such as Figure 6 would likely be barely detectable.

The most important point illustrated by Figure 6 is that the electric field pattern (i.e., the sequence of signs) is basically the same under very quiet conditions as during disturbed conditions (Note: treating the weak field between $2^{\text{h}0^{\text{m}}}$ and $2^{\text{h}3^{\text{m}}}$ UT as an exception to this statement would be misleading in terms of other examples). This is consistent with studies which have shown that the basic pattern, and pattern variability, of high latitude magnetic disturbance vectors is not dependent on disturbance level (Harang, 1946; Heppner, 1972). The electric field measurements thus reinforce arguments (Heppner, 1969) against theories which treat the existence and/or sign of dawn-dusk polar cap electric fields in terms of the direction of interplanetary magnetic fields.

(C) High latitude nightside traverses (N. Hemi.)

Figure 7 illustrates several typical features for orbits that cross to the magnetic nightside of the north pole and to the magnetic dayside of the south pole. These are successive passes during a three hour period with $K_p = 4$. Considering here the northern high latitudes, there are two features

to note. One is the low magnitude in the auroral belt. With the assumption that the north (late evening) and south (early morning) fields at these local times are comparable to those at 18^h and 6^h, the low magnitude is what is expected for the measured component perpendicular to the sun-earth line (i.e., the northeast and southeast components, respectively, as labelled in Figure 7).

The other feature of note is the roughly monotonic increase in the $|-E_X|$ polar cap field between the late evening and early morning hours. This is probably not solely attributable to the X-axis orientation. The magnitudes, $|-E_X|$, reached on the early morning (i.e., near 4^h MLT) side of the polar cap are large compared to average polar cap magnitudes along other orbits. This indicates that the convection is faster poleward from the auroral belt between 2^h and 5^h MLT than it is in other regions of the nightside polar cap. This characteristic of the polar cap field is not always confined to the nightside (2 - 5^h); many N. hemisphere 18^h - 6^h MLT traverses also show a maximum $|-E_X|$ on the morning side (i.e., near 6^h MLT) of the polar cap. Statistically the tendency for the maximum $|-E_X|$ to occur near 6^h in passes from 18^h to 6^h is almost as common as having a roughly constant $-E_X$ across the polar cap as shown previously in Figures 4 and 5. The large field reversals emphasized by Cauffman and Gurnett (1971) appear to correspond to cases where $|-E_X|$ has a trough-like maximum adjacent to the $+E_X$ auroral belt (as defined in the "Introduction").

(D) High latitude dayside traverses (S. Hemi.)

The traverse after 23^h30^m UT in Figure 7 (bottom curve) is roughly between 6^h40^m and 17^h40^m MLT and comes close to the magnetic pole. The sequence of equatorward → dawn-dusk → poleward fields is normal but as noted previously the

field shows more roughness than in N. polar regions. The traverse following 21^h50^m UT in Figure 7 (2nd curve) from approximately 7^h30^m to 16^h50^m MLT is slightly more to the dayside with a maximum Λ of 84° near noon. In this example one cannot objectively pick a polar cap boundary in the pre-noon hours; instead the field is rather chaotic. In the afternoon hours a region of dawn-dusk field is encountered followed by a more normal evening auroral belt field.

In most cases, the pre-noon dayside field is considerably more chaotic (or turbulent) than the field in the afternoon hours. The traverse shown in Figure 8 illustrates this characteristic more strikingly than the Figure 7 examples. Here the pass is roughly from 8^h30^m to 15^h30^m MLT with a maximum Λ of about 75° near noon. Polar cap boundary identification is meaningless and the only resemblance to polar passes occurs in the afternoon where the auroral belt field appears relatively normal.

(E) Boundary locations

Designating a low latitude boundary for the auroral belt convection is often somewhat subjective as the reader can judge from examining examples given. Roughly the criteria used here correspond to having deflections from the lower latitude measurements exceeding about 5 volts/km although in some cases the appearance of irregularity structures in other data channels influences the selection. Auroral belt-polar cap boundaries are more readily picked, by definition, where the sign reverses and remains reversed for a large distance. Also as defined "boundaries" can be sharp, suggesting the existence of a shear, or gradual, suggesting a transition with local convective continuity. Both are called boundaries for purposes here.

Figure 9 illustrates the distribution of boundary locations for three levels of magnetic activity. Each plot is for a different day: a disturbed

day when the average 3-hour Kp was 4, the next for a day with an average Kp of 2, and the third for a day with an average Kp of 1. The coordinates are magnetic time and invariant latitude. N. and S. hemisphere points were first plotted separately to note any systematic differences in the latitude-time regions where they overlap. As differences were not apparent they were combined. However, very few polar cap-auroral belt boundaries could be clearly designated in the S. hemisphere dayside region discussed in the previous section. Thus, these do not appear and some traverses are not represented as a consequence of missing data in critical regions. It is apparent that there is considerable variability in the boundary locations; however by discarding a small fraction of the points, particularly those near the pole, this impression changes. A tendency for polar cap and low latitude boundaries to be separated less on the morning side than on the evening side is evident. This is more clear in Figure 10.

Figure 10 shows the average boundary locations along the N. hemisphere 18^h to 6^h meridian using only data that fit the selective criteria stated on the figure. Only 3-hour Kp levels of 2, 3, and 4 are shown because the number of crossings fitting the selection criteria at other disturbance levels is not adequate for comparable statistical significance. The most noteworthy feature in Figure 10 is the 12 to 14° width of the evening auroral belt. This is wider than anticipated from studies of magnetic disturbance vectors (e.g., Heppner, 1969). The morning auroral belt is narrower, $\Delta \Lambda = 8$ to 12°. Another point of interest is that at 6^h the average latitude of the polar cap boundary does not decrease with increasing levels of magnetic disturbance as it does for the other boundaries.

(F) Locations of maximum field strength

Figure 11 illustrates the N. hemisphere locations where peak field intensities, maximum $|E_X|$, were encountered for two levels of disturbance, $K_p = 1$ and $K_p = 4$. Only one point is plotted for each zone (evening-polar cap-morning) for a given satellite traverse. The distribution is only meaningful relative to the distribution of orbits in magnetic coordinates in the N. hemisphere (illustrated by Figure 3) and must carefully be viewed with this in mind. Several features are, however, apparent. One, is that the latitude of maximum E_X in the auroral belt is much more variable under $K_p = 4$ conditions than when K_p is 1. A related general feature is that maximum intensities in the auroral belt occur most frequently in the high latitude portions of the belt. Another characteristic, consistent with the discussion under (C) above, is that the maximum polar cap fields, $| -E_X |$, on the nightside occur predominantly in the early morning hours but near the $18^h - 6^h$ meridian the maximum $| -E_X |$ is likely to be found almost anywhere along the polar traverse. The location of maximum $| -E_X |$ in the polar cap does not appear to be very dependent on the level of magnetic disturbance.

UNUSUAL FIELD DISTRIBUTIONS

Calling a field distribution "unusual" involves a highly subjective judgment. Degrees of variance from the most commonly observed field distributions cannot be readily defined and are necessarily related to the scale examined. Here we are concerned only with the overall profile of a polar crossing. Figure 12 is somewhat unique in that it permits illustration of large scale variances in both the N. and S. hemispheres from successive traverses.

The non-typical characteristic in the N. hemisphere pass from 18^h to 6^h MLT (Figure 12) is the reversal back to a + E_x region poleward from a - E_x region that normally would be considered to be within the polar cap. Also, the morning auroral belt field encountered later on this traverse is unusually weak.

The non-typical characteristic in the S. hemisphere pass from about 5^h40^m to 18^h MLT is the highly erratic field, with numerous field reversals, extending to roughly the midnight meridian from the morning side. If this pass had been on the dayside this behavior would not have been considered unusual in terms of the previous discussion (Section D, above). In effect, the unusual distribution in Figure 12 might be considered to be a consequence of the morning dayside region of irregular fields expanding spatially toward the night hours.

An interesting aspect of the Figure 12 examples is that the non-typical behavior occurs in completely different local time regions, evening and morning, respectively, in the N. and S. hemispheres even though the measurements are separated by only one-half an orbital period. A general statement that applies to practically all non-typical features is that they are seen only in an isolated region of a given traverse; seldom, if ever, is the field unusual throughout a polar traverse. This point is re-emphasized by the substorm examples in the next section.

FIELD BEHAVIOR DURING SUBSTORM EVENTS

The term "substorm" has been used in different context by different people. The terms "polar elementary storm" and "bay disturbances" are usually equivalent to "substorm." Here, "substorm" merely means a period of enhanced magnetic activity at auroral latitudes. As discussed elsewhere (Heppner, 1972)

one can be somewhat more precise by referring to individual bay enhancements within a more general period of activity. For example, only rarely can the beginning or end of a disturbed period be clearly defined but it is often possible to clearly define sudden onsets of negative bays even though their occurrences are dependent on the previous existence of disturbance. Thus, the sudden onset of a negative bay is taken to be an event within a substorm. In some usages this would be called the onset of a substorm; as long as the dual meanings are recognized and magnetograms are shown the physical situation, if not the semantics, should be clear. All the examples previously shown, except Figure 6, occurred during substorm activity; thus, the substorm field does not differ from the typical field. More specifically, below, the electric field behavior preceding, during, and following the occurrence of sudden negative bay onsets is examined.

First, considering times prior to the sudden onset of a negative bay (called the growth phase of a substorm by some investigators) the general consistency of the pattern of high latitude electric fields statistically suggests that major differences in the electric field distribution are not likely to be found. This is confirmed by preliminary examination of individual cases to the extent that one can conclude that if there are significant differences, these differences must be subtle and not immediately recognizable. Figure 13 provides an example. The magnetogram shows a sudden bay onset at 5^h19^m UT. The N. polar traverse shown at the top of the figure occurred during 15 minutes preceding the onset. There is nothing particularly unusual about the field distribution with the possible exception of noting that the maximum in the $|-E_x|$ polar cap does not statistically occur frequently in the evening region. Attaching importance to this deviation would be highly speculative.

The same magnetogram, Figure 13, relative to another traverse, serves to illustrate behavior in the polar cap during a sudden onset and in the morning auroral belt immediately following a sudden onset. The sudden onset occurs at 8^h29^m UT which is just after the satellite has passed through the evening auroral belt (Figure 13, center) and is located near 18^h30^m MLT and $\Lambda = 77^\circ$. There is no evidence of any peculiar behavior at the onset time and the remainder of the traverse is quite normal.

Next, two examples are given for cases where the sudden negative bay onset occurs minutes before the satellite passes through the evening auroral belt to polar cap transition. In the first example, Figure 14, the sudden onset (4^h23 - 4^h25^m UT, Great Whale and Churchill observatories) occurs while the satellite is in the S. hemisphere morning auroral belt. The field distribution along this traverse, slightly to the nightside of the pole, is relatively normal until the region of transition between the polar cap and the evening auroral belt is approached. Proceeding toward lower latitudes, from roughly 19^h MLT and $\Lambda = 77^\circ$, a region of very large fluctuations is encountered and this is then followed by a relatively normal evening auroral belt field. The peak magnitudes and numerous sharp field reversals between $\Lambda = 71^\circ$ and 76° are definitely not typical.

The second example, Figure 15, illustrates that the effects associated with the negative bay onset can be even more spatially isolated and reach greater magnitudes than the Figure 14 example. The negative bay began sharply at 7^h49^m UT (Churchill magnetogram) during a period of considerable disturbance as indicated by the large $+\Delta H$ variation at College, Alaska. At this time the satellite was entering the N. hemisphere evening auroral belt. The auroral belt field is not particularly unusual but the field in a narrow zone at the

polar cap boundary is highly disturbed in terms of several sharp field reversals and large peak magnitudes. The remainder of the traverse across the polar cap and morning auroral belt is relatively normal.

From examination of data throughout the various phases of large negative bays it appears that the unusual behavior at the evening auroral belt-polar cap boundary occurs only during the early stages of the negative bay event while $|\Delta H|$ is increasing. The overall significance of this correlation, and the lack of correlation in other regions contacted by OGO-6, is not clear at this stage of analysis. The important point for the present is that these abnormal fluctuations are seen only in an isolated region.

DISCUSSION

This presentation of OGO-6 measurements in a sense represents a progress report; it is apparent that the measurements provide a base for future analyses ranging from fine structure studies to the construction of global convection patterns. The data from numerous high latitude Ba^+ drift studies is in excellent agreement with the OGO-6 measurements and these two bodies of data are highly complementary. The OGO-6 measurements allow one to see how the various regional Ba^+ measurements fit into more global patterns and in turn the 3-dimensional pictures of \underline{E} vs. time from multiple Ba^+ clouds allow one to see how the electric field varies with time in selected regions. A comprehensive discussion is beyond the scope of this presentation but it is interesting to see how the OGO-6 designations "auroral belt" and "polar cap" fit into previous studies.

Figure 16 permits comparison with a diagram (left side, Figure 16) the author was using prior to the OGO-6 results. It is based primarily on: (a) analyses of magnetic disturbance conducted prior to 1968, and (b) OV1-10

satellite data which gave a low latitude boundary for the auroral belt convection (Heppner, 1969). However, the information for drawing a dawn-dusk polar cap field came from more recent Ba^+ drift studies in the polar cap (Heppner et al., 1971). The comparison, left and right sides of Figure 16, shows that the average low latitude boundaries for auroral belt convection agree very well. The principal difference is in the location of the polar cap boundary. The average boundary, where determined, between the auroral convection and the polar convection is at a higher latitude near the twilight meridian than the boundary estimated from magnetic disturbance vectors. Alternatively, one can say that the belt of auroral convection from OGO-6 is considerably wider than pictured previously near the twilight meridian. The difference between diagrams decreases in moving toward midnight from the twilight hours. The previous picture agrees with OGO-6 in terms of showing a narrower auroral belt near 6^h than near 18^h.

The OGO-6 measurements clearly illustrate that selecting an average or typical location for the polar cap boundary on the dayside is not very meaningful because of its variability. A similar, difficulty was noted (Heppner, 1969) in drawing the previous picture (left side, Figure 16). With the OGO-6 measurements it becomes necessary to drop speculative boundaries and thus a dayside polar cap boundary is not shown for OGO-6 in Figure 16.

As indicated on Figure 16, the sum of the potential drops across the auroral belt at 6^h and 18^h is approximately equal to the drop across the polar cap, based on rather crude integrations and ignoring altitude changes. More precise integrations in the future will test the accuracy of the equality and its variability from orbit to orbit. The integrated change in potential across the polar cap is nearly always within the range 20 to 100 kilovolts. The most typical values for moderate disturbance conditions (such as $K_p = 3$) are in the center of this range--roughly 40 to 70 kilovolts.

Figure 17 conveniently summarizes the spatial association of several characteristics discussed, relative to the average boundaries of Figure 16. Reasons for the special characteristics of sub-regions, and reasons for differences in detail between the N and S polar regions, cannot be divorced from a more general understanding of the forces responsible for the overall convective pattern and such interpretations are outside the scope of this presentation. The most important single conclusion that is apparent at this date is that the high latitude electric field pattern is not highly variable and that when unusual variations occur they are relatively isolated in time and spatial extent. This result contradicts models which envoke major changes in the electric field configuration to explain substorms.

Acknowledgement

The OGO-6 electric field experiment was conducted by T. L. Aggson, N. C. Maynard, and the author. The author is indebted to his co-workers for their many efforts in making this presentation possible.

REFERENCES

- Aggson, T. L. and Heppner, J. P. (1964). A proposal for electric field measurements on ATS-1, NASA-GSFC Report, July 1964.
- Cauffman, D. P. and Gurnett, D. A. (1971). Double-probe measurements of convection electric fields with the Injun-5 satellite, J. Geophys. Res., 76, 6014-6027.
- Cauffman, D. P. and Gurnett, D. A. (1972). Satellite measurements at high latitude convection electric fields, Space Sci. Rev. (to be published).
- Föppel, H., Haerendel, G., Haser, L., Lüst, R., Melzner, F., Meyer, B., Neuss, N., Rabben, H., Rieger, E., Stöcker, J., and Stoffregen, W. (1968). Preliminary results of electric field measurements in the auroral zone, J. Geophys. Res., 73, 21-26.
- Frank, L. A. and Gurnett, D. A. (1971). Distributions of plasmas and electric fields over the auroral zones and polar caps, J. Geophys. Res., 76, 6829-6846.
- Haerendel, G. (1971). Electric fields and their effects in the ionosphere, Proc. of the "International Symposium on Solar Terrestrial Physics," Leningrad, May 1970 (to be published).
- Haerendel, G. and Lüst, R. (1970). Electric fields in the ionosphere and magnetosphere, Particles and Fields in the Magnetosphere (Ed. B. M. McCormac) D. Reidel Publ. Co., Dordrecht, 213-228.
- Harang, L. (1946). The mean field of disturbance of polar geomagnetic storms, Terr. Mag., 51, 353-380.
- Heppner, J. P. (1969). Magnetospheric convection patterns inferred from high latitude activity, Atmospheric Emissions (Eds. B. M. McCormac and A. Omholt) Van Nostrand Reinhold Co., 251-266.
- Heppner, J. P., Stolarik, J. D., and Wescott, E. M. (1971). Electric field measurements and the identification of currents causing magnetic disturbances in the polar cap, J. Geophys. Res., 76, 6028-6053.

- Heppner, J. P. (1972). The Harang discontinuity in auroral belt ionospheric currents, Geofys. Publ., Minneskrift for Prof. L. Harang (Eds. J. Holtet and A. Egeland) Universitetsforlaget, Oslo (to be published).
- Maynard, N. C. (1972). Electric fields in the ionosphere and magnetosphere, Proc. of the "Advanced Study Institute on Magnetosphere-Ionosphere Interaction," Dalseter, Norway, April 1971 (to be published).
- Maynard, N. C. and Heppner, J. P. (1970). Variations in electric fields from polar orbiting satellites, Particles and Fields in the Magnetosphere (Ed. B. M. McCormac) D. Reidel Publ. Co., Dordrecht. 247-253.
- Wescott, E. M., Stolarik, J. D., and Heppner, J. P. (1969). Electric fields in the vicinity of auroral forms from motions of barium vapor releases, J. Geophys. Res., 74, 3469-3487.
- Wescott, E. M., Stolarik, J. D., and Heppner, J. P. (1970). Auroral and polar cap electric fields from barium releases, Particles and Fields in the Magnetosphere (Ed. B. M. McCormac) D. Reidel Publ. Co., Dordrecht. 229-238.

FIGURE CAPTIONS

- Figure 1: Illustration of OGO-6 showing the locations of the symmetric electric field probes.
- Figure 2: OGO-6 orbit plane perpendicular to noon-midnight plane in June 1969.
- Figure 3: (caption on figure)
- Figure 4: Typical E_X along successive traverses across the N and S polar regions.
- Figure 5: Typical E_X for two N polar traverses
- Figure 6: E_X for a N polar traverse during very quiet magnetic conditions ($K_p = 0$)
- Figure 7: Successive N and S hemisphere traverses when the dipole tilt places the satellite on the night and day sides, respectively, of the N and S magnetic poles.
- Figure 8: A S hemisphere high latitude (non-polar) dayside traverse
- Figure 9: Locations of auroral belt and polar cap convection boundaries for three days having different levels of magnetic activity: solid dots represent the low latitude boundary of auroral belt convection, open circles mark the boundary between the evening auroral belt and the polar cap, crosses mark the boundary between the morning auroral belt and the polar cap. For the meaning of "boundary" see text.
- Figure 10: (caption on figure)
- Figure 11: (caption on figure)
- Figure 12: Successive N and S polar traverses showing unusual field behavior in the evening polar cap (N hemisphere) and morning polar cap (S hemisphere).

Figure 13: (1) A N polar traverse (top curve) preceding a sudden negative bay onset at 5^h 19^m UT. (2) A N polar traverse (middle curve) during which a sudden negative bay onset occurred, 8^h 29^m UT.

Figure 14: A S polar traverse immediately following the occurrence of a sudden negative bay onset, 4^h 23^m - 4^h 25^m UT.

Figure 15: A N polar traverse immediately following the occurrence of a sudden negative bay onset at 7^h 49^m UT.

Figure 16: Comparison of average convection boundaries for Kp = 3: previous picture (left side), OGO-6 measurements (right side).

Figure 17: Locations of sub-regions having special characteristics.

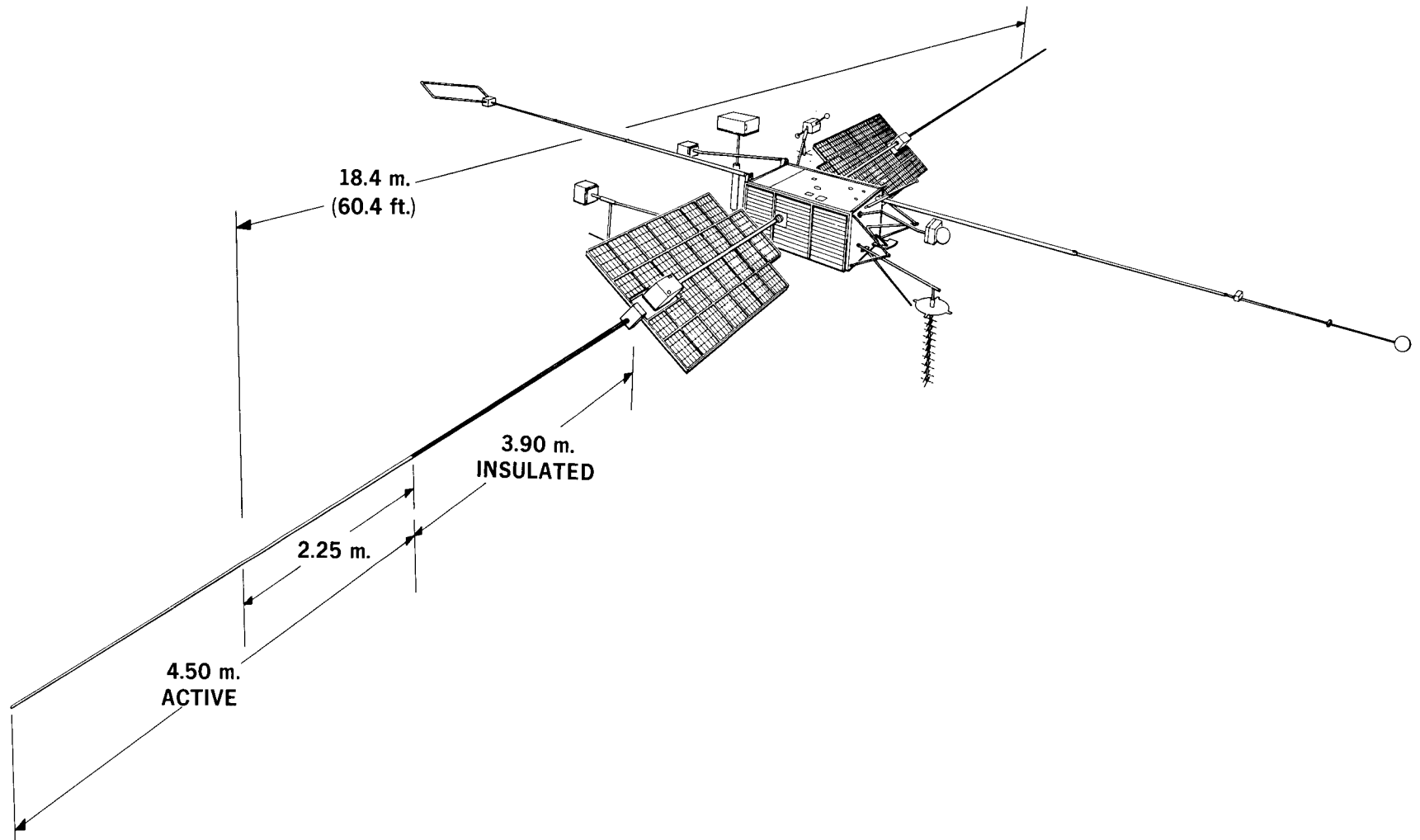


FIGURE 1

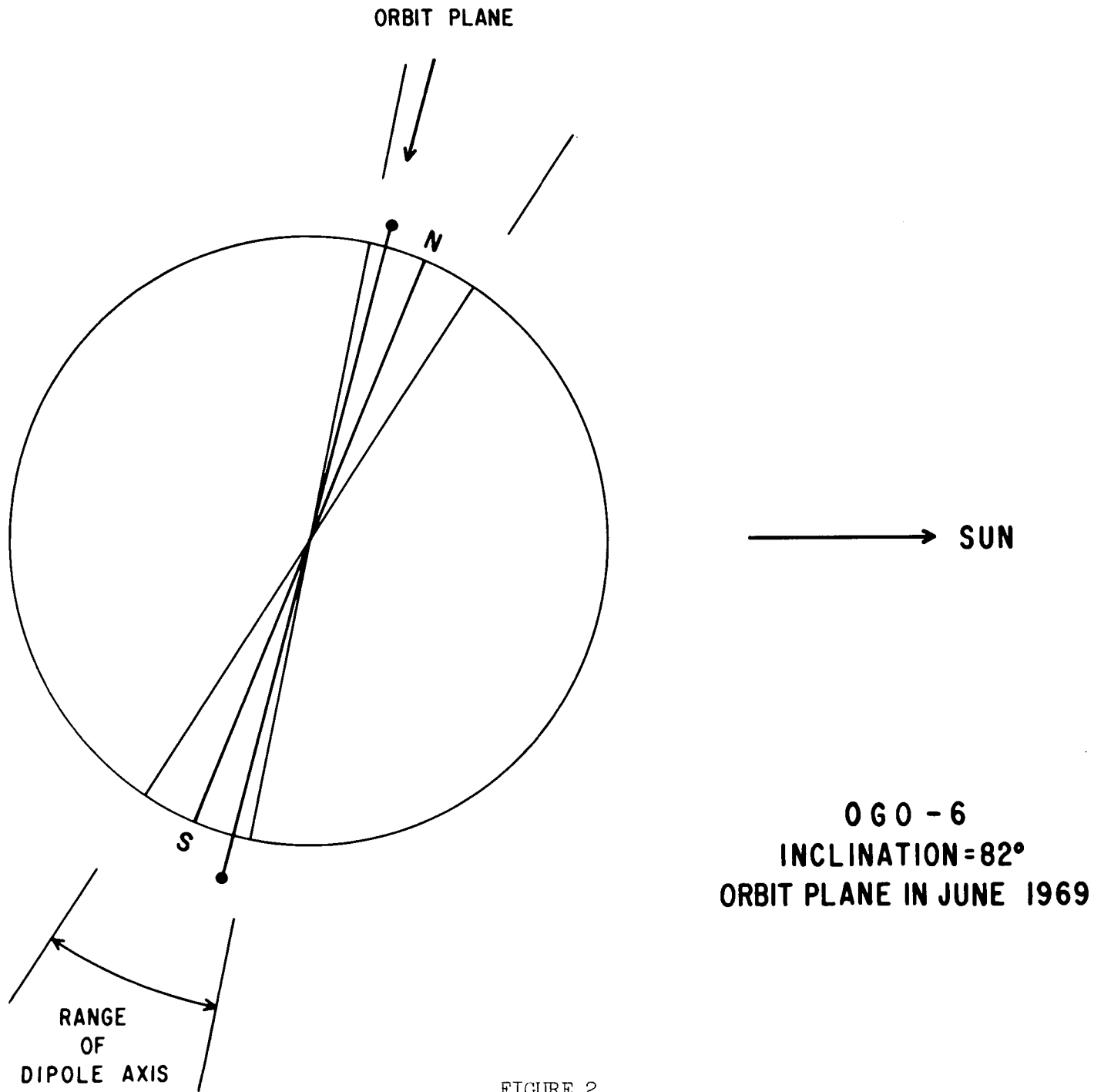
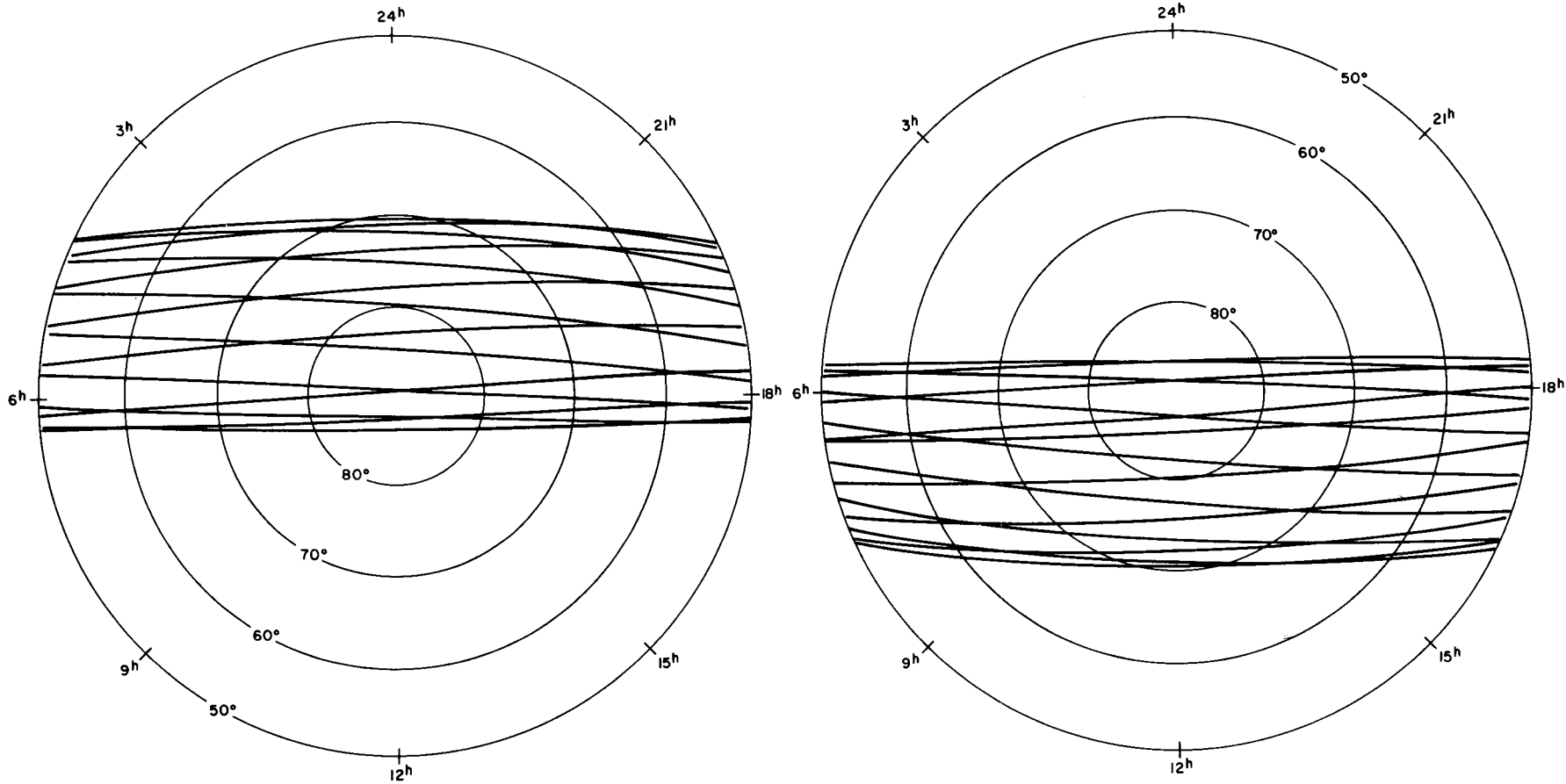


FIGURE 2

NORTH POLAR REGION

SOUTH POLAR REGION



**OGO-6 POLAR COVERAGE DURING A 24^h PERIOD: JUNE 14, 1969
IN
MAGNETIC LATITUDE vs. MAGNETIC TIME COORDINATES**

FIGURE 3

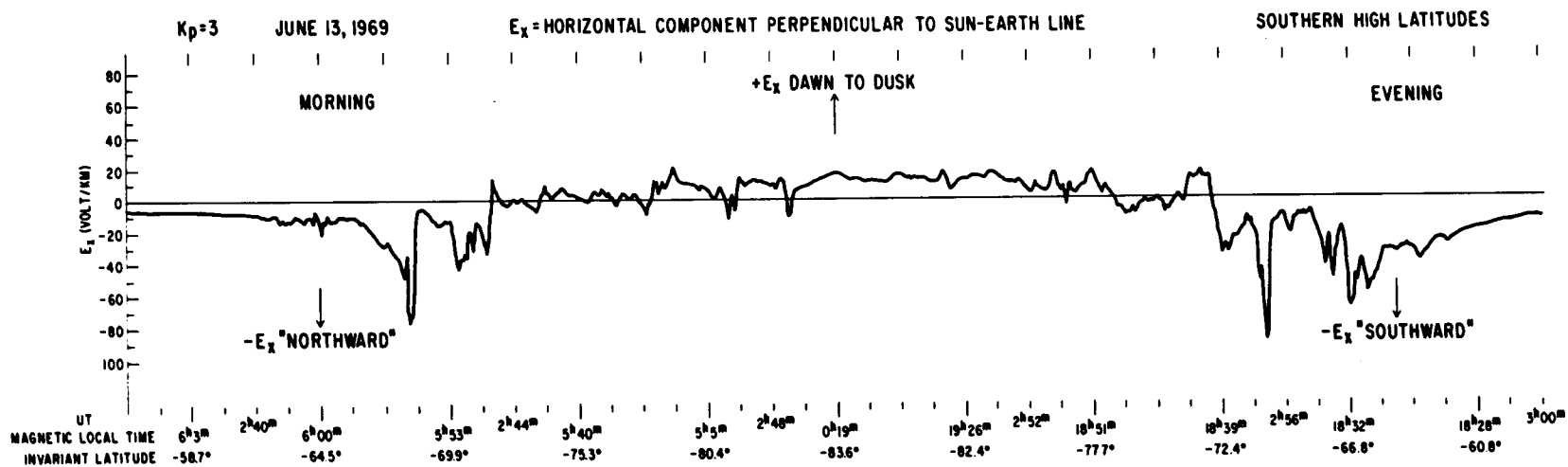
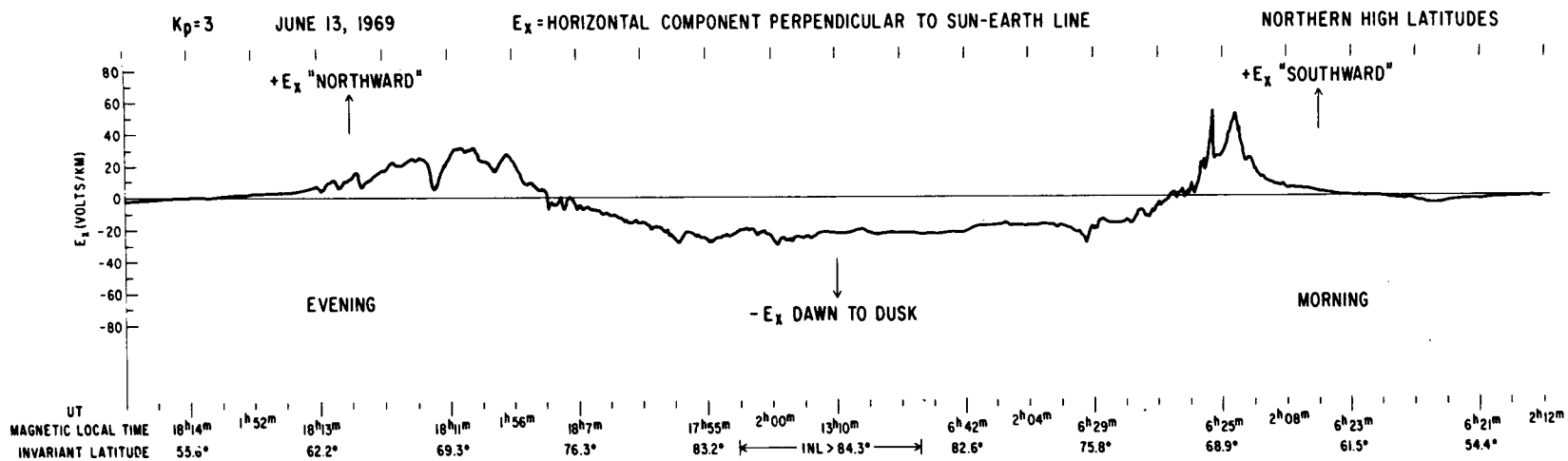
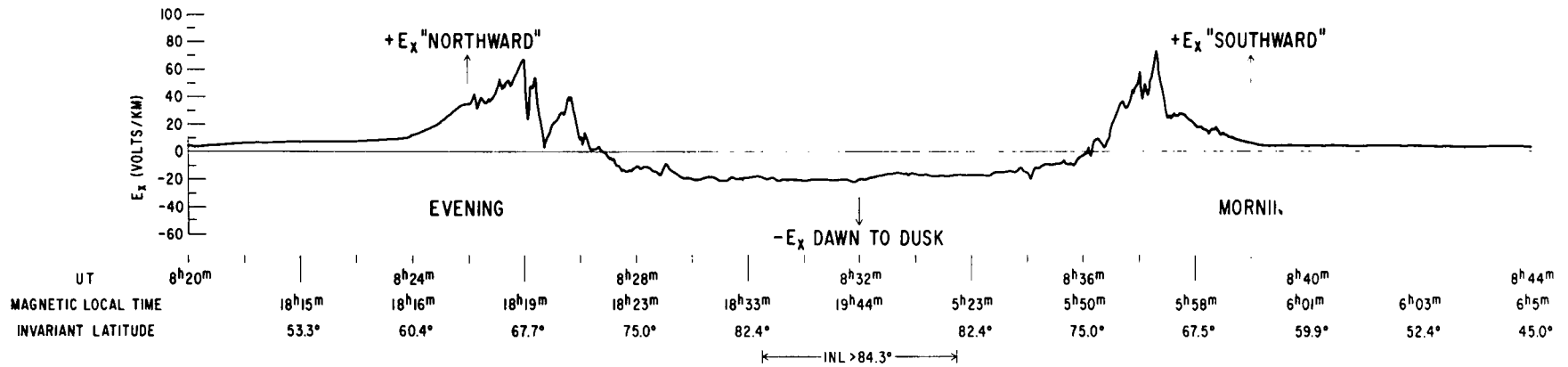


FIGURE 4

(Kp=3-) JUNE 11, 1969 E_x=HORIZONTAL COMPONENT PERPENDICULAR TO SUN-EARTH LINE NORTHERN HIGH LATITUDES



(Kp=4-) JUNE 12, 1969 E_x=HORIZONTAL COMPONENT PERPENDICULAR TO SUN-EARTH LINE NORTHERN HIGH LATITUDES

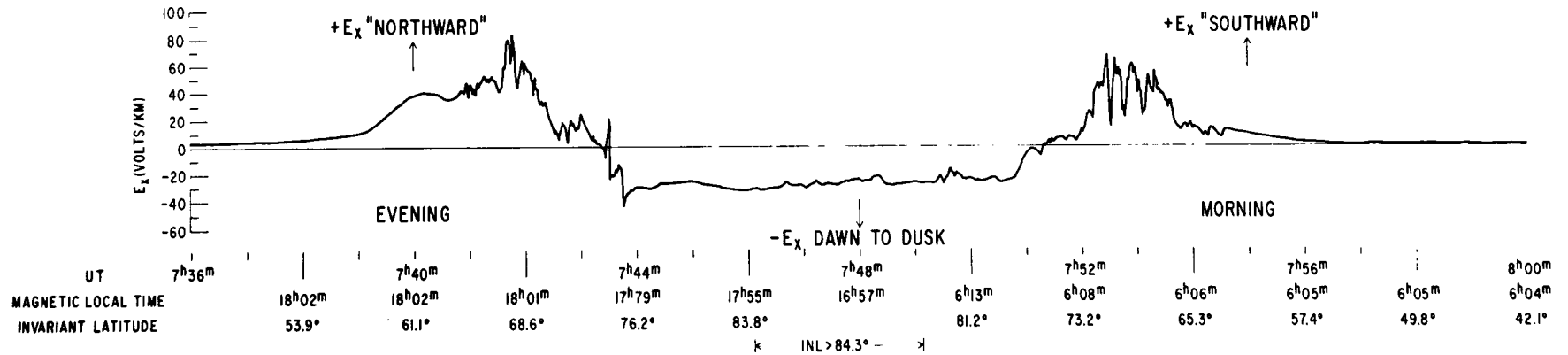


FIGURE 5

(Kp=0) JUNE 22, 1969 E_x = HORIZONTAL COMPONENT PERPENDICULAR TO SUN-EARTH LINE NORTHERN HIGH LATITUDES

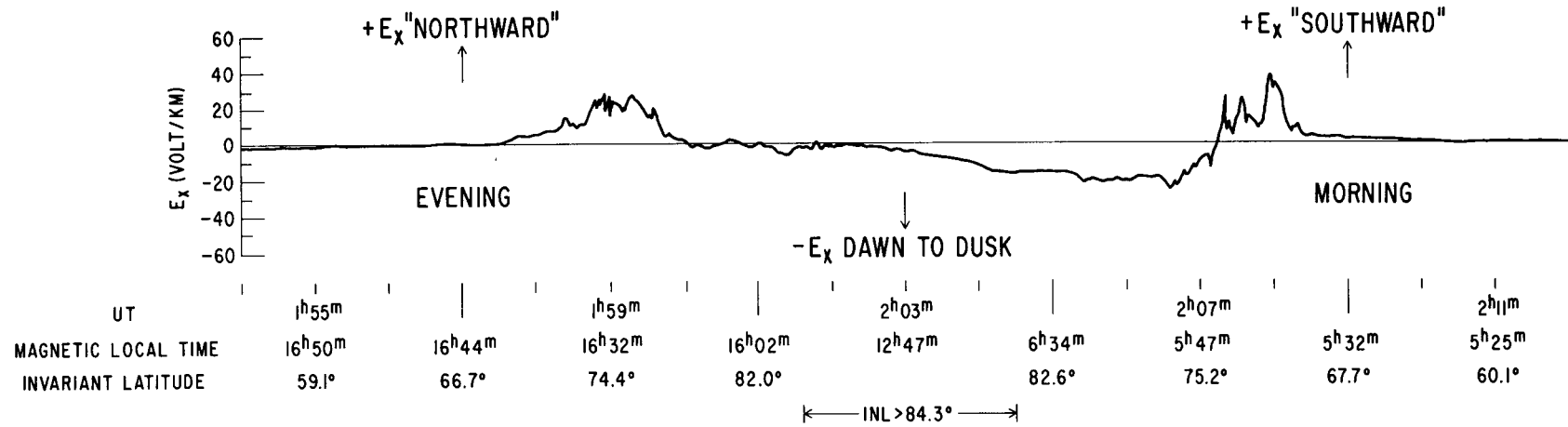


FIGURE 6

($K_p=4$) 21^h-24^h, JUNE 14, 1969 E_x =HORIZONTAL COMPONENT PERPENDICULAR TO SUN-EARTH LINE

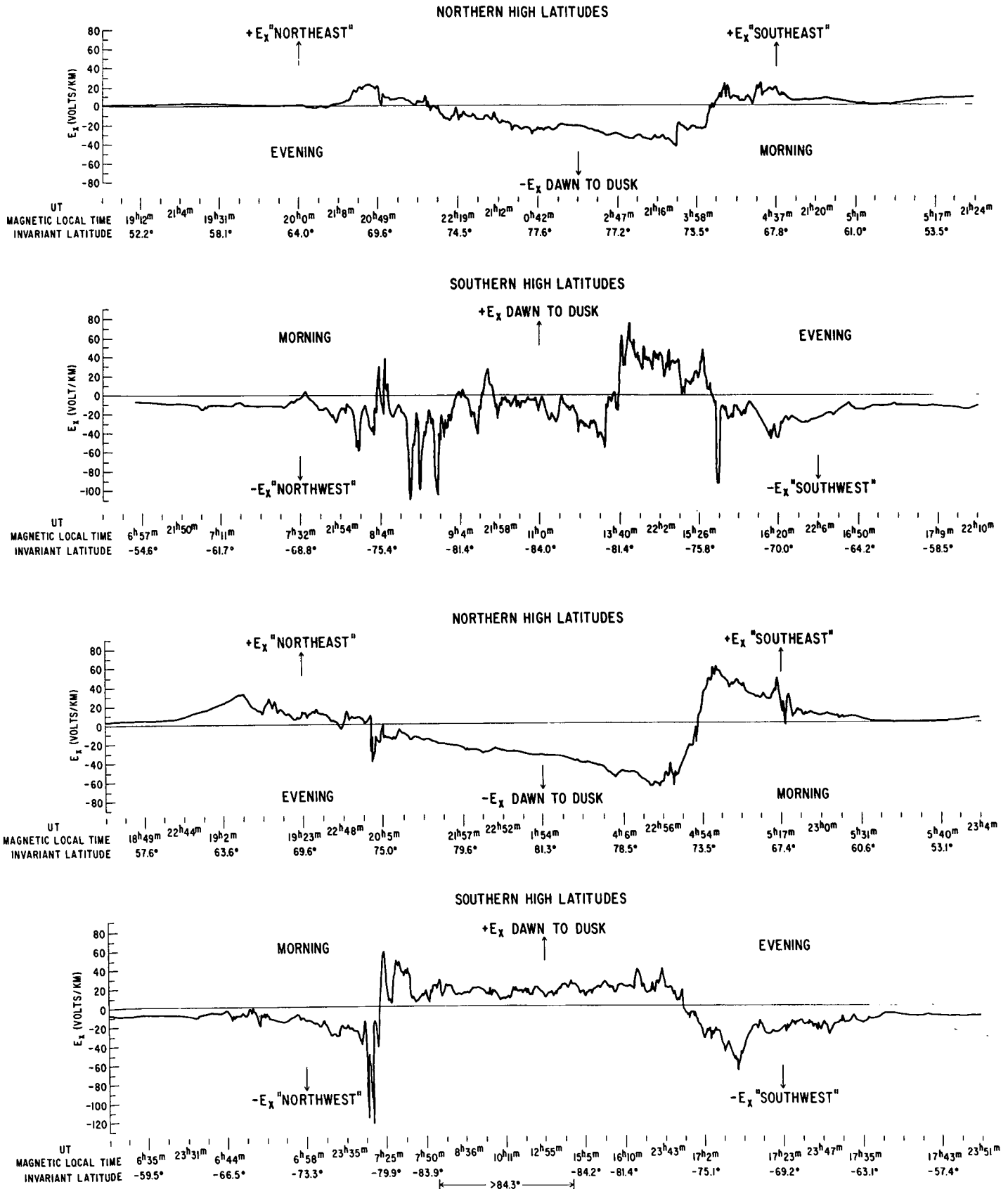


FIGURE 7

(K_p=3) JUNE 13, 1969 E_x=HORIZONTAL COMPONENT PERPENDICULAR TO SUN-EARTH LINE

SOUTHERN HIGH LATITUDES

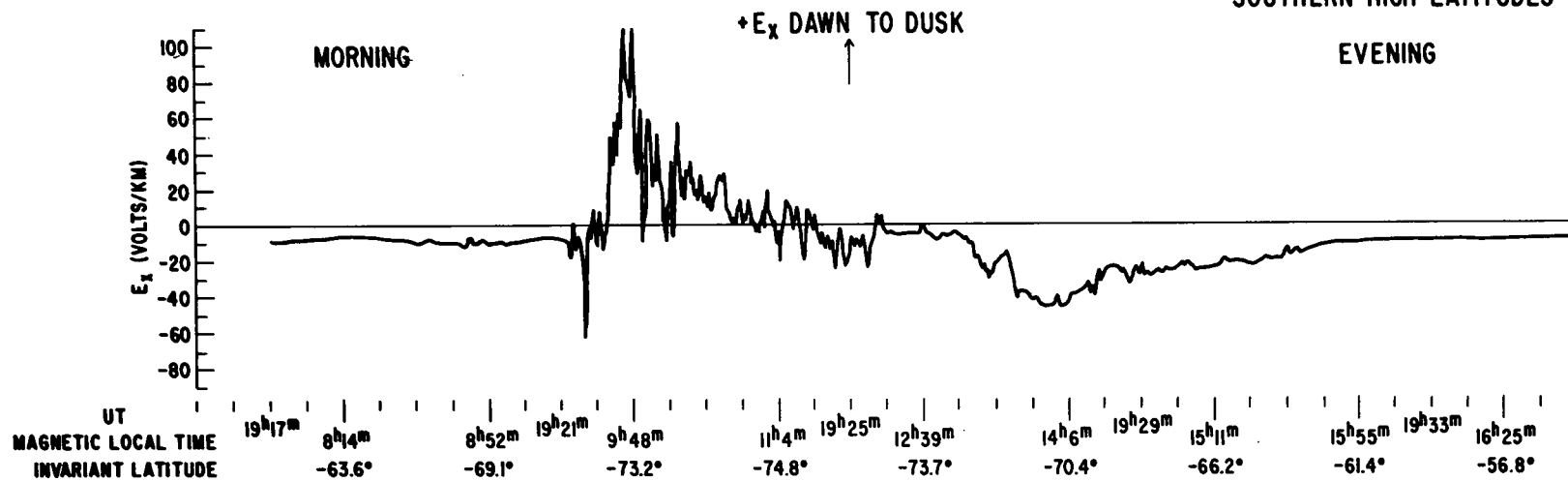
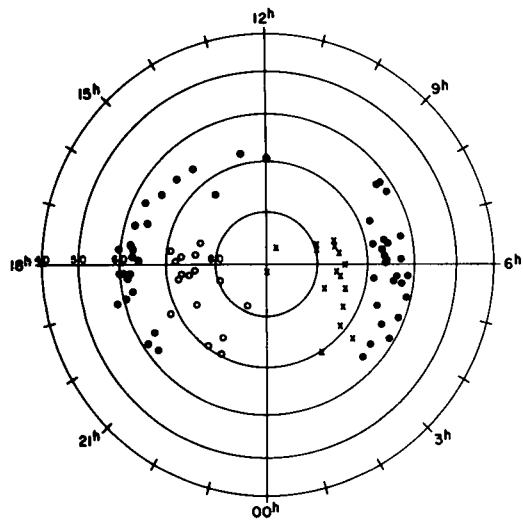
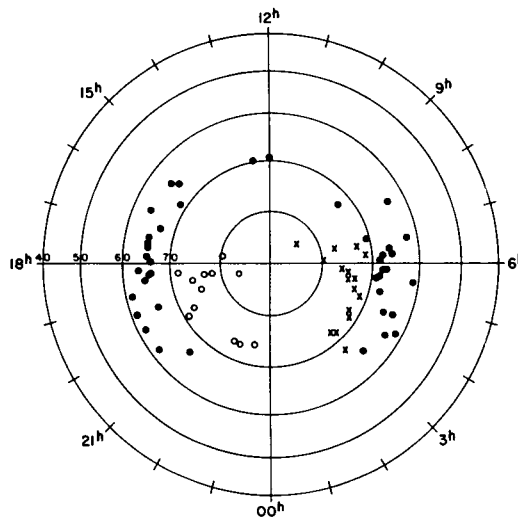


FIGURE 8

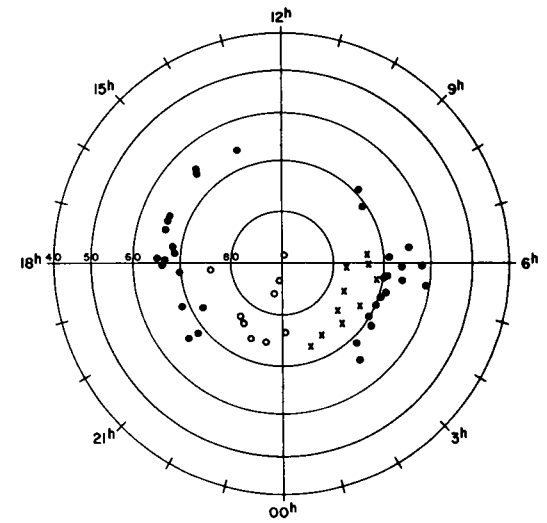
LOCATIONS OF AURORAL BELT AND POLAR CAP BOUNDARIES



JUNE 14, 1969
 3-HOUR K_p RANGE: 3⁻ TO 6⁻
 DAILY K_p SUM: 33



JUNE 15, 1969
 3-HOUR K_p RANGE: 2⁻ TO 3⁻
 DAILY K_p SUM: 17



JUNE 18, 1969
 3-HOUR K_p RANGE: 0⁺ TO 2⁻
 DAILY K_p SUM: 8

SYMBOLS:
 ● $E_x \rightarrow O$ LOW LATITUDE BOUNDARY
 ○ $+E_x \rightarrow -E_x$ "EVENING"
 x $-E_x \rightarrow +E_x$ "MORNING"

FIGURE 9

AVERAGE "AURORAL BELT" BOUNDARIES AT 18^h AND 6^h MAGNETIC TIME
 FROM N. HEMI. PASSES CONFINED TO 18^h±1^h AND 6^h±1^h AND COMPLETE
 FOR ALL FOUR BOUNDARY POINTS PER POLAR PASS

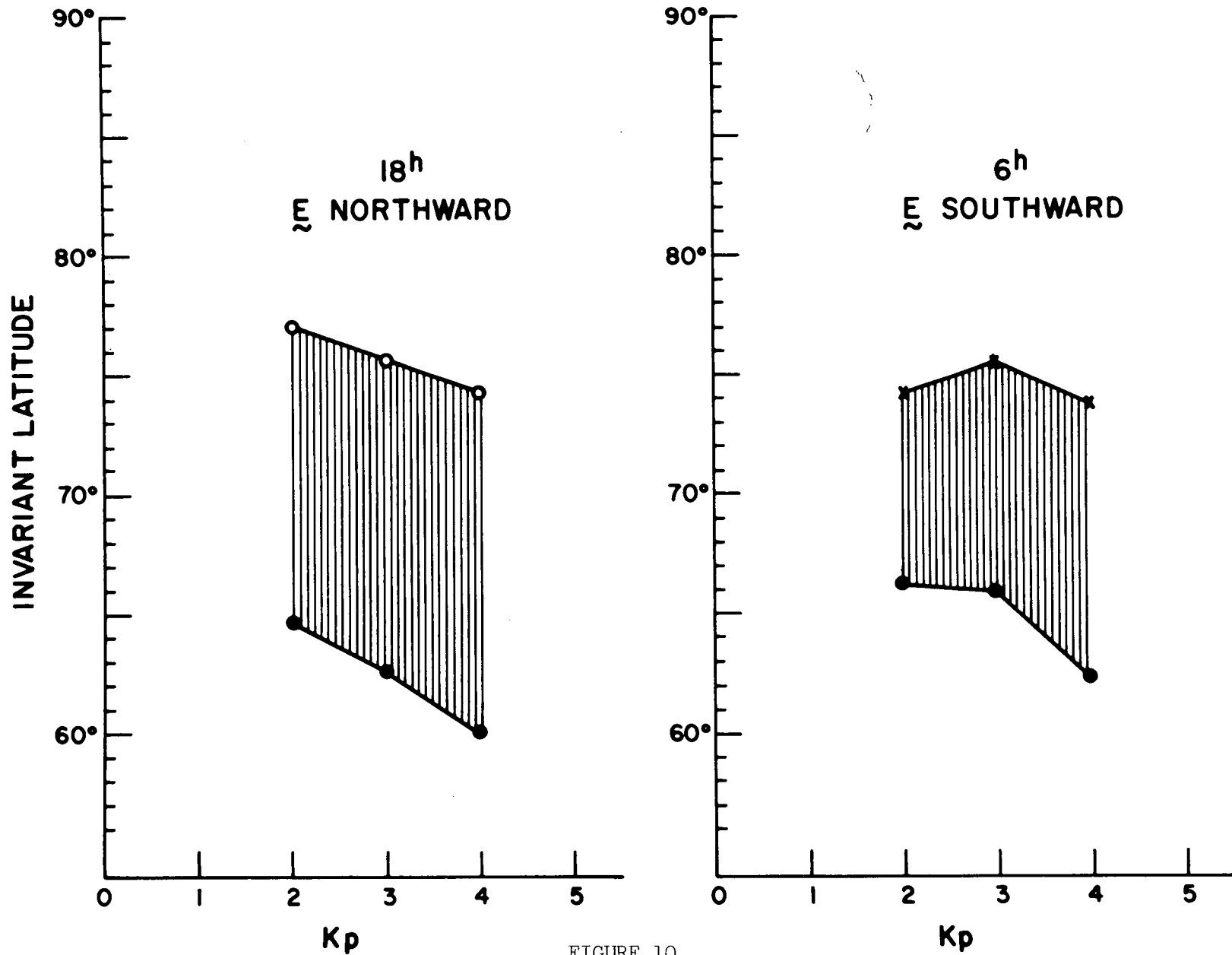
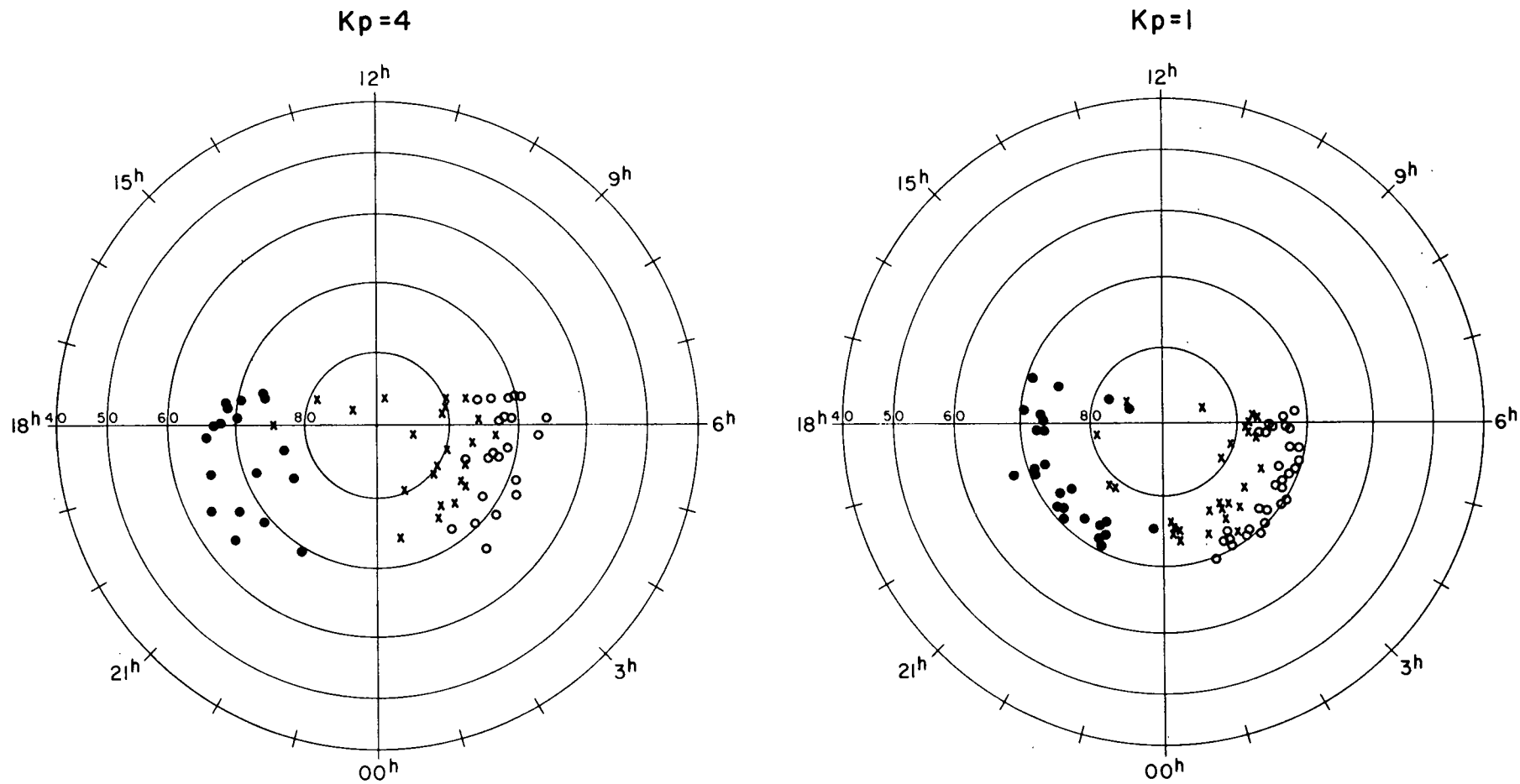


FIGURE 10

LOCATIONS OF $|E_x|$ MAXIMUMS PER SATELLITE PASS
(NORTHERN HEMISPHERE)



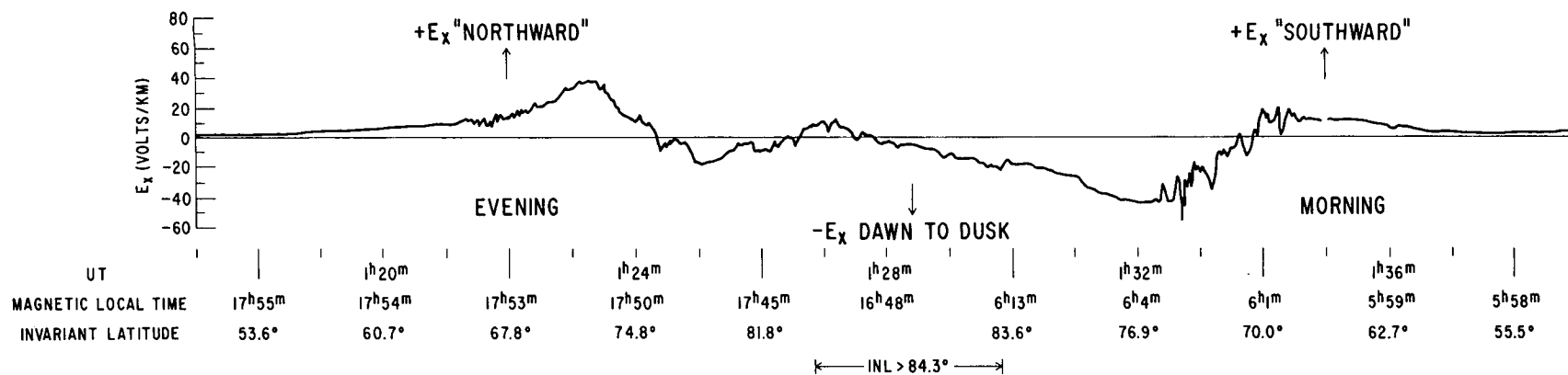
SYMBOLS:

- $+E_x$ (EVENING)
- x $-E_x$ (POLAR)
- $+E_x$ (MORNING)

FIGURE 1.1

(Kp=3⁻) JUNE 16, 1969 E = HORIZONTAL COMPONENT PERPENDICULAR TO SUN-EARTH LINE

NORTHERN HIGH LATITUDE



(Kp=3⁻) JUNE 16, 1969 E_x = HORIZONTAL COMPONENT PERPENDICULAR TO SUN-EARTH LINE

SOUTHERN HIGH LATITUDES

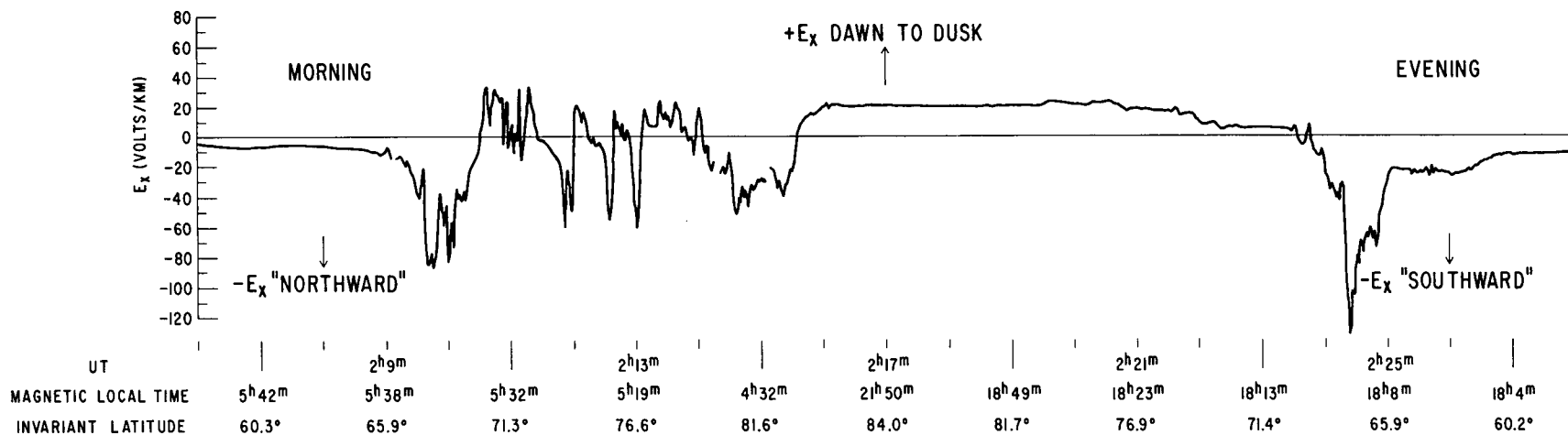
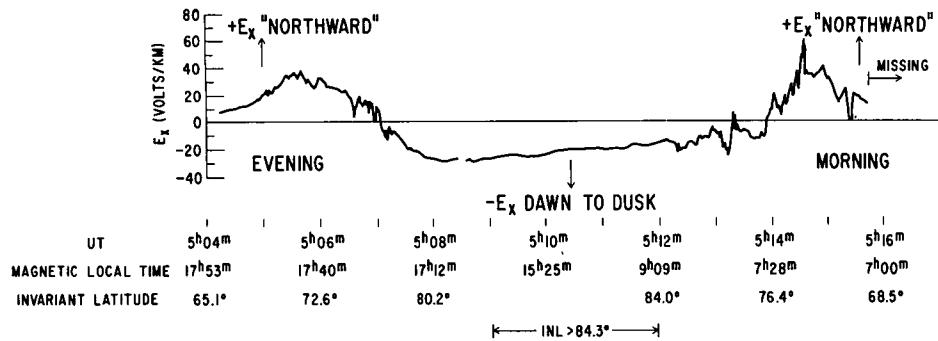


FIGURE 12

(Kp=2-) JUNE 11, 1969 E_x=HORIZONTAL COMPONENT PERPENDICULAR TO SUN-EARTH LINE
NORTHERN HIGH LATITUDES



(Kp=3-) JUNE 11, 1969 E_x=HORIZONTAL COMPONENT PERPENDICULAR TO SUN-EARTH LINE
NORTHERN HIGH LATITUDES

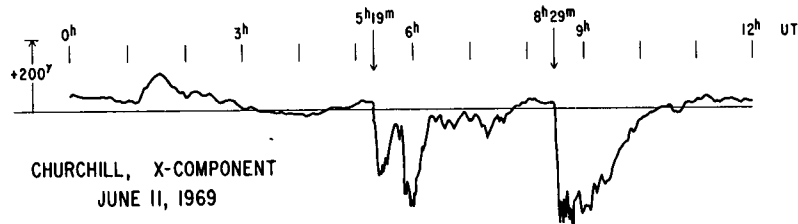
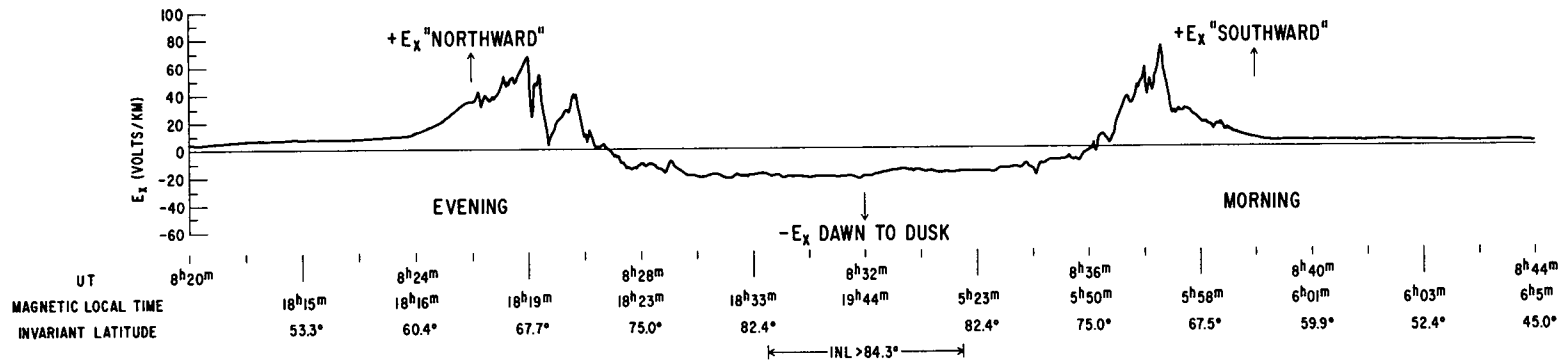


FIGURE 13

(K_p=4) JUNE 13, 1969 E_x=HORIZONTAL COMPONENT PERPENDICULAR TO SUN-EARTH LINE

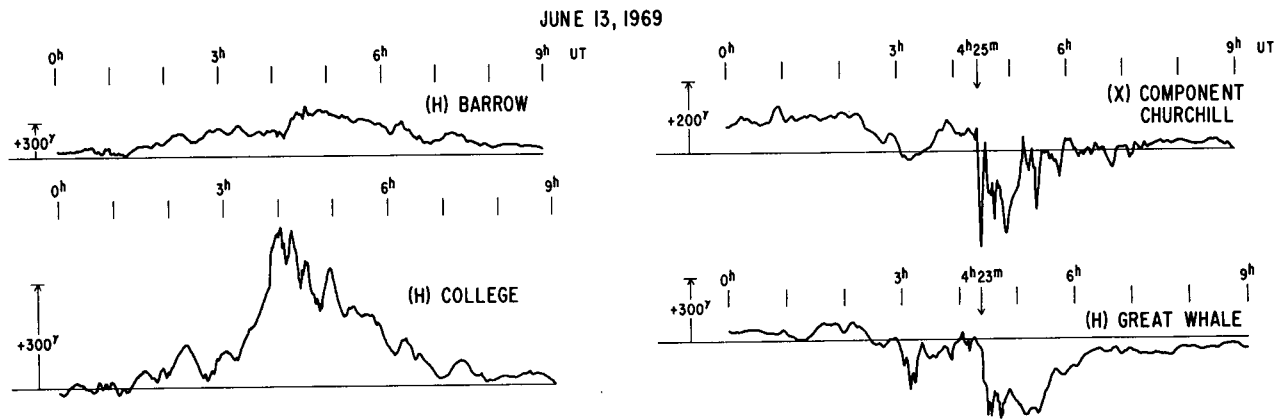
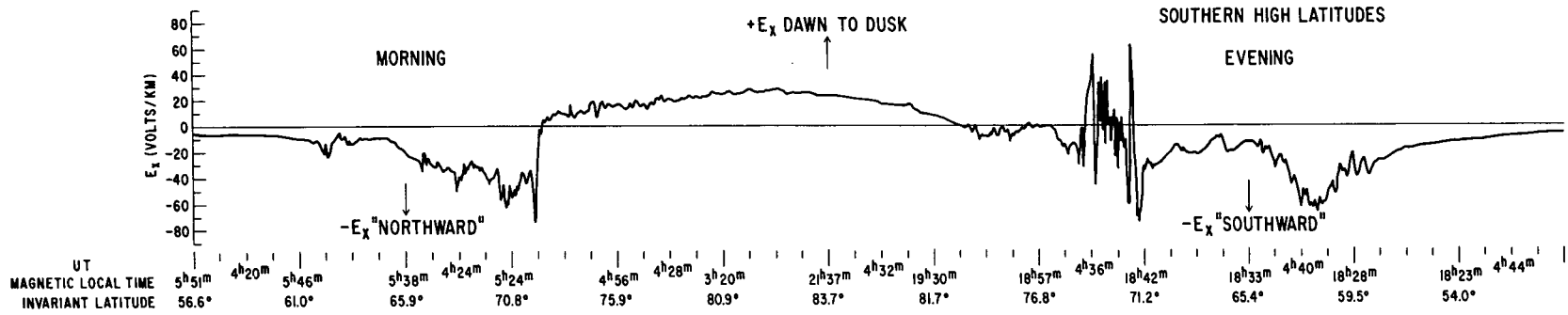


FIGURE 14

(Kp=5) JUNE 14, 1969 E_x = HORIZONTAL COMPONENT PERPENDICULAR TO SUN-EARTH LINE NORTHERN HIGH LATITUDES

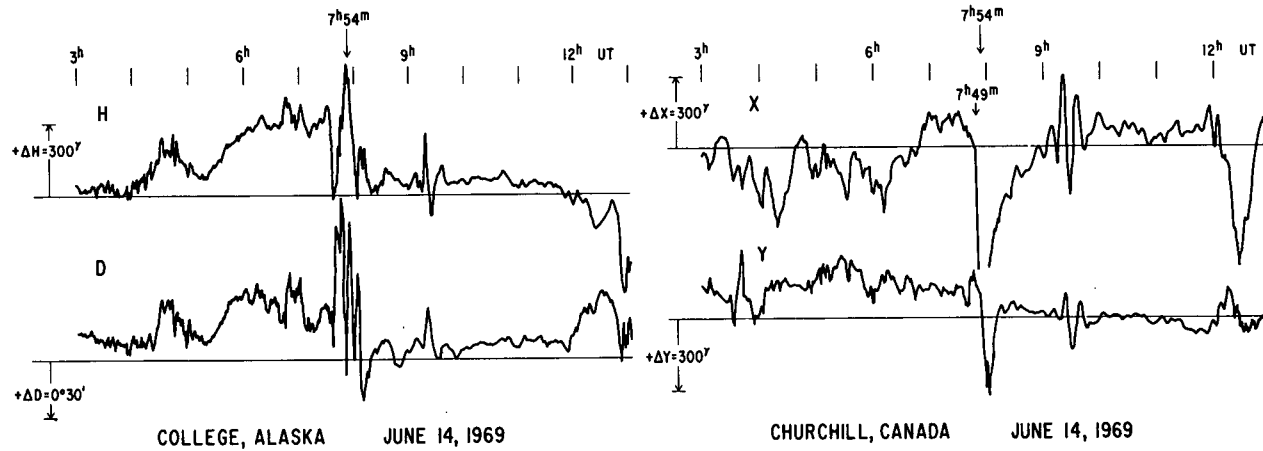
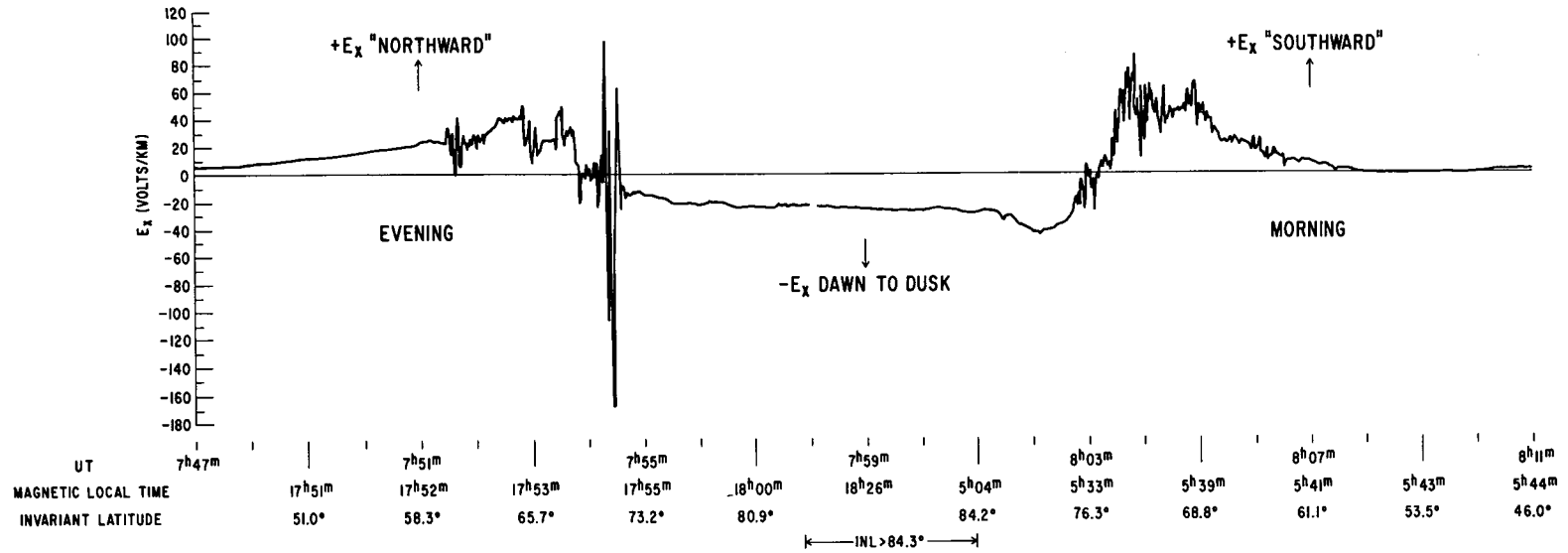
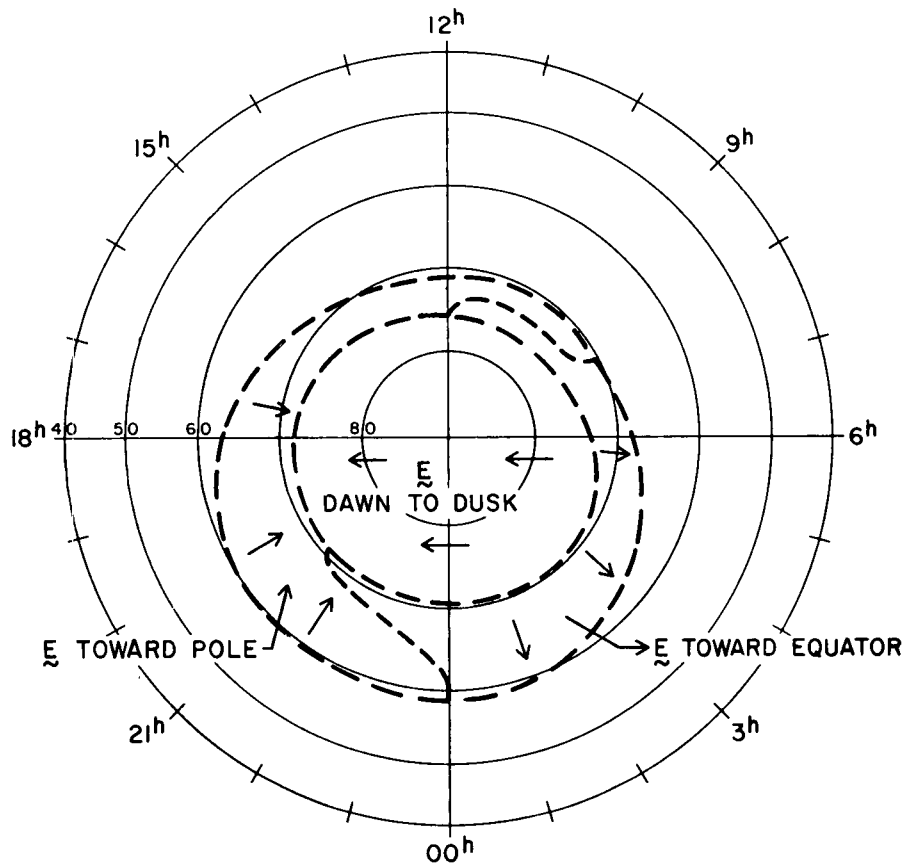
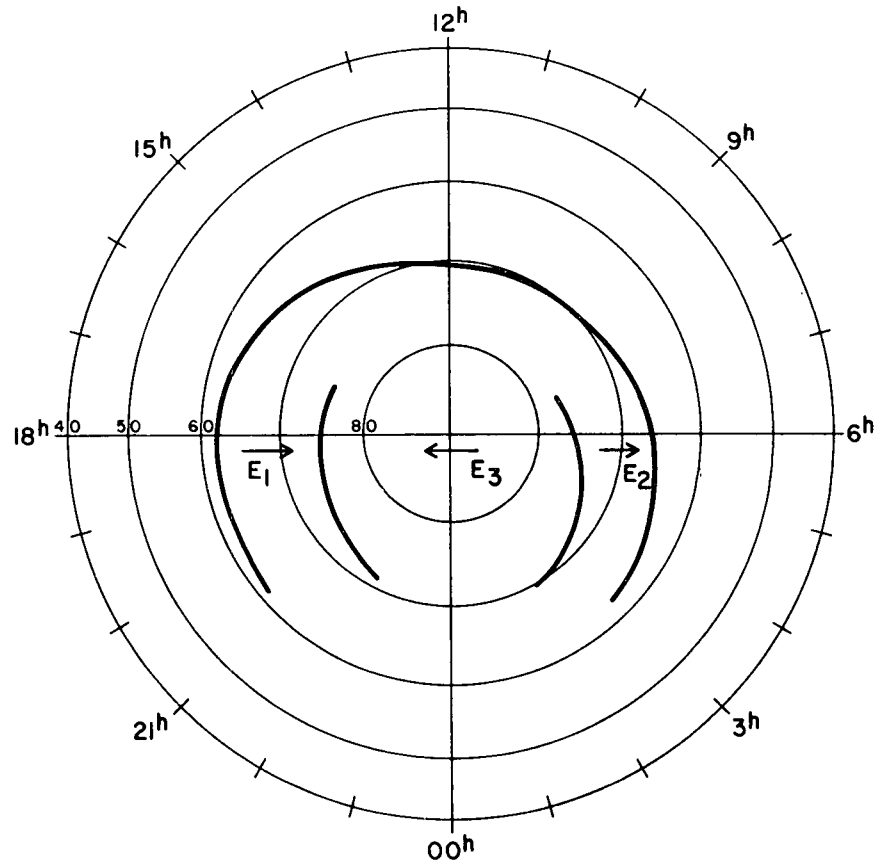


FIGURE 15

"AURORAL" AND "POLAR CAP" CONVECTION BOUNDARIES
($K_p \approx 3$)

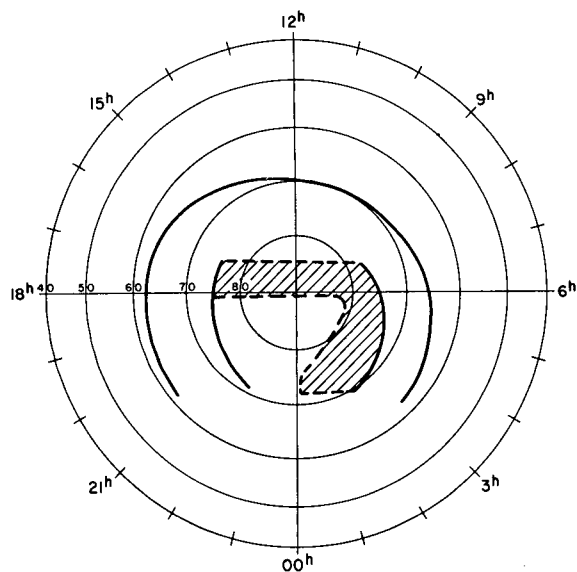


OLD
MAGNETIC DISTURBANCE ANALYSIS (\rightarrow 1968)
OVI-10 SATELLITE (1967)
 Ba^+ RELEASES (1967 \rightarrow)

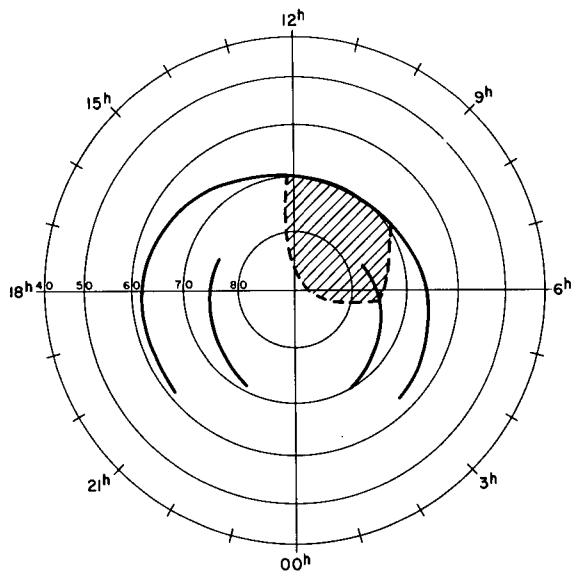


OGO-6
 $W = \text{WIDTH OF REGION}$
 $\bar{E}_3 W_3 \approx \bar{E}_1 W_1 + \bar{E}_2 W_2$
TYPICALLY $\bar{E}_3 W_3$ IN CENTER OF
RANGE 20 TO 100 KILOVOLTS

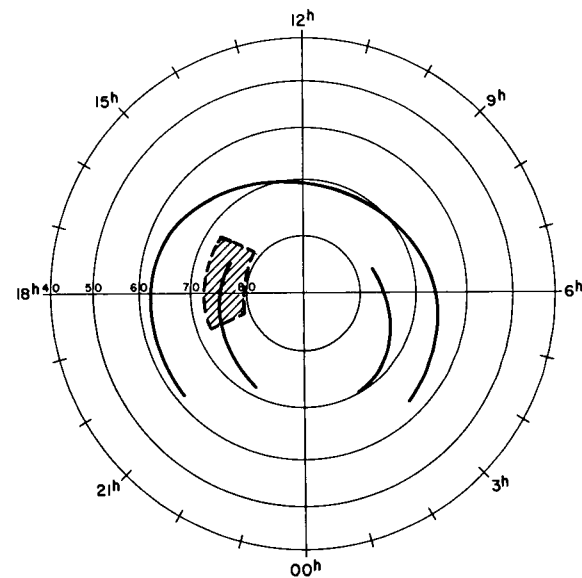
FIGURE 16



(A) NORTHERN HEMISPHERE REGION OF MAXIMUM
POLAR CAP $|E_x|$ FOR OGO-6 ORBITS:
JUNE 1969



(B) SOUTHERN HEMISPHERE REGION OF
FREQUENT REVERSALS OF THE SIGN OF E_x
(i.e., $-E_x \rightarrow +E_x \rightarrow -E_x \dots$) JUNE 1969



(C) REGION OF LARGE FLUCTUATIONS AND SIGN
REVERSALS DURING INCREASING $|\Delta H|$ NEAR
MIDNIGHT FOLLOWING THE SUDDEN ONSET
OF A NEGATIVE BAY (BOTH HEMISPHERES)

FIGURE 17